THE JOURNAL OF PHYSICAL CHEMISTRY B

Article

pubs.acs.org/JPCB

Interaction of G-Quadruplex with RecA Protein Studied in Bulk Phase and at the Single-Molecule Level

Atsushi Tanaka,[†] Jungkweon Choi,*[,†] Seog K. Kim,[‡] and Tetsuro Majima*[,†]

[†]The Institute of Scientific and Industrial Research (SANKEN), Osaka University, Mihogaoka 8-1, Ibaraki, Osaka 567-0047, Japan

[‡]Department of Chemistry, Yeungnam University, Gyeongsan City, Gyeong-buk, 712-749, Republic of Korea

Supporting Information

ABSTRACT: As in the human genome there are numerous repeat DNA sequences to adopt into non-B DNA structures such as hairpin, triplex, Z-DNA, G-quadruplex, and so on, an understanding of the interaction between DNA repair proteins and a non-B DNA forming sequence is very important. In this regard, the interaction between RecA protein and human telomeric 5′-TAGGG-$(TTAGGG)_3$-TT-3′ sequence and the G-quadruplex formed from this sequence has been investigated in bulk phase and at the single-molecule level. The RecA@ssDNA filament, which is formed by the interaction between RecA protein and a G-rich sequence, was dissociated by the addition of K^+ ions, and the dissociated G-rich sequence was quickly folded to a G-quadruplex structure, indicating that the G-quadruplex structure is more favorable than the RecA@ssDNA filament in the presence of K^+ ions. In addition, we demonstrate that the conformation of the G-quadruplex, which is heterogeneous in the absence of RecA, converged to the specific G-quadruplex with one double-chain-reversal loop upon association of RecA protein.

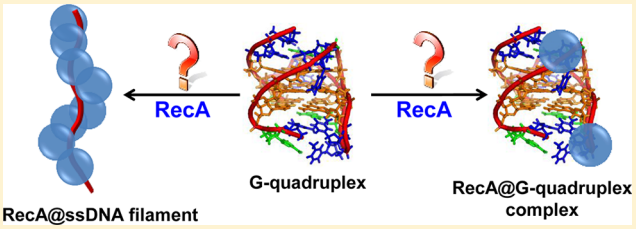

1. INTRODUCTION

Biopolymers, such as protein, DNA, and so on, perform their functions through the interaction with other biopolymers in living cells; for example, protein−protein interaction, protein−DNA interaction, and so on. The protein−DNA interaction especially plays an important role in biological processes such as DNA replication, recombination, repairing of damaged DNAs and gene transcription. Thus, an elucidation of a protein−DNA interaction occurring in physiological conditions is a prerequisite for understanding such a biological process. Among various protein−DNA interactions, the interaction between DNA repair proteins such as RecA family proteins and single-stranded DNA (ssDNA) has received much attention in the biological and biomedical fields. The RecA family of proteins such as Rad51 and RecA catalyze a DNA strand exchange reaction between ssDNA and homologous double-stranded DNA (dsDNA), the so-called homologous recombination (HR).[1−4] The primary function of HR is to maintain genome stability during vegetative growth of prokaryotic cells or mitosis of eukaryotic cells. In this HR reaction, RecA protein (or Rad51) binds to ssDNA in an ATP-dependent manner and then forms a helical nucleofilament.[5−7] In this regard, the interaction between RecA protein and ssDNA/dsDNA has been extensively investigated in bulk phase[4,8,9] and at the single-molecule level.[3,10−13]

However, most studies on RecA-DNA interaction have been performed on ssDNA, which can form a B-DNA duplex with Watson−Crick base pairing. Generally, it is known that repeat DNA sequences occupy more than 50% of the total genomic DNA.[14] Under a certain condition, these repetitive DNA sequences are major contributors to the formation of non-B DNA structures including hairpins, triplexes, Z-forms, G-quadruplexes, i-motifs, and so on.[15−17] Furthermore, these non-B DNA-forming sequences can induce genetic instability and consequently may cause human disease.[16,18] Especially, it is known that in vitro, G-quadruplex, which is formed from a guanine (G)-rich sequence in the presence of monovalent cations such as K^+ and Na^+ ions, can affect celluar DNA replication and transcription, and influence genomic stability.[15,19−22] Thus, G-quadruplex has been regarded as a signpost and controller for the oncogene expression at the transcription level. Practically, there have been numerous attempts that exploit the G-quadruplex structure as therapeutic targets as well as a drug carrier in biomedical applications.[23−25] Recently, Balasubramanian and co-workers showed that G-quadruplex formation in human cells is modulated during cell-cycle progression and that endogenous G-quadruplex structures can be stabilized by a small-molecule ligand.[26] These findings provide substantive evidence for G-quadruplex formation in the genome of mammalian cells and the importance of the intermolecular interaction in living cells. In this sense, an understanding of the interaction between a protein and a non-B DNA forming sequence such as a G-rich sequence is very important.

Here, we have investigated the interaction between RecA protein and a G-rich sequence in bulk phase and at the single-

Received: April 12, 2013
Revised: May 6, 2013

   dx.doi.org/10.1021/jp4036277 | J. Phys. Chem. B XXXX, XXX, XXX−XXX

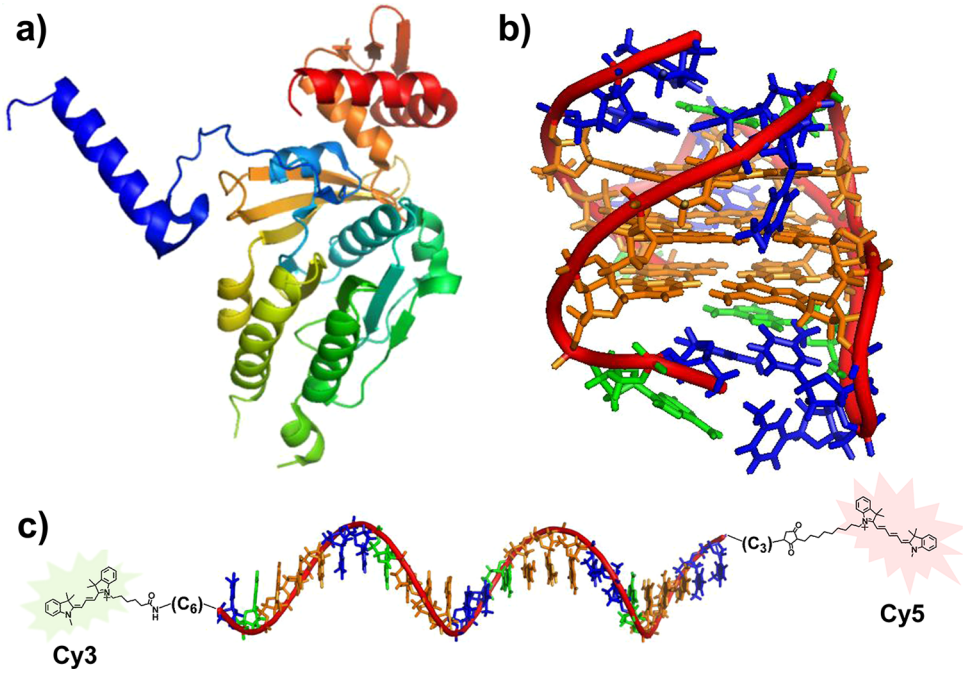

Figure 1. (a) Structure of RecA protein (PDB ID: 1G19). (b) G-quadruplex with one double-chain-reversal loop (PDB ID: 2JSL; guanine, thymine, and adenine are colored orange, blue, and green, respectively.). (c) Human telomeric sequence adopted in this study, Cy5−5′-TAGGG-$(TTAGGG)_3$-TT-3′-Cy3 (**Cy5-G-q-Cy3**). Cy5 and Cy3 are attached to the 5′- and 3′-ends, respectively, for the FRET experiment. Guanine, thymine, and adenine are colored orange, blue, and green, respectively.

molecule level. In this study, we used *Escherichia coli* RecA protein and dye-labeled human telomeric sequence (Cy5-5′-TAGGG-$(TTAGGG)_3$-TT-3′-Cy3, **Cy5-G-q-Cy3**, Figure 1). *E. coli* RecA, which is homologous to the Rad51 protein, is a ∼38 kDa multifunctional DNA-binding protein (Figure 1a).[27] The results presented here show that upon addition of K^+ ions, RecA@ssDNA filament, which is formed by the interaction between RecA protein and the G-rich single-stranded sequence in the absence of K^+ ions, is dissociated, and then the dissociated G-rich single-stranded sequence is quickly folded to a G-quadruplex structure. This observation suggested that the G-quadruplex structure is more favorable than RecA@ssDNA filament in the presence of K^+ ions. In addition, we found that RecA protein binds preferentially to G-quadruplex with one double-chain-reversal loop. Furthermore, G-quadruplex formed from the human telomeric sequence (5′-TAGGG-$(TTAGGG)_3$-TT-3′, **G-q**), whose conformation is heterogeneous in the physiological condition, changes its conformation to G-quadruplex with one double-chain-reversal loop upon interaction with RecA protein. To our best knowledge, this is the first report for the interaction between RecA protein and G-quadruplex DNA studied in bulk phase and at the single-molecule level.

2. EXPERIMENTAL METHODS

Full experimental details and characterization of compounds can be found in the Supporting Information. All sample solutions were prepared with 10 mM Tris-HCl buffer (pH 7.4) In all experiments carried out with the single-stranded G-rich sequence, magnesium ions were not added to the sample solutions because magnesium ions induce the aggregation of the single-stranded G-rich sequence (data not shown).

The steady-state UV−visible absorption, fluorescence, and circular dichroism (CD) spectra were measured using a Shimadzu UV-3100, a Horiba FluoroMax-4, and JASCO CD-J720, respectively. All fluorescence spectra were measured with an excitation wavelength of 532 nm. On the other hand, it is difficult to measure the CD signal with high concentration of the protein (10 μM) because the absorption in the far-UV region is too high. Therefore, we measured all CD signals with a 0.1 mm path-length cell to decrease the absorption in the far-UV region. On the other hand, in order to elucidate the change in CD signal of DNA upon addition of RecA, the CD signal of the RecA sample was measured and then compared to the CD signal of a DNA and RecA mixture sample. From the comparison of the two CD signals, we found that the CD signal of RecA was not affected by the formation of the RecA@DNA complex. On the basis of this result, we subtracted the CD signal of RecA from the CD signal of the DNA and RecA mixture sample. Fluorescence correlation spectroscopy (FCS) experiments for ssDNA and G-quadruplex in the absence and presence of *E. coli* RecA at room temperature were measured with a time-resolved fluorescence microscope using confocal optics (MicroTime 200; PicoQuant, Berlin-Adlershof, Germany).

In order to measure the fluorescence resonance energy transfer (FRET) efficiency of freely diffusing ssDNA and G-quadruplex in the absence and presence of *E. coli* RecA at the single-molecule level, 3.6 nM sample solutions were prepared. Single-molecule FRET (smFRET) experiments were carried out with the same confocal optics (MicroTime 200; PicoQuant, Berlin-Adlershof, Germany) and two single photon avalanche photodiodes (Micro Photon Devices, PDM 50CT and 100CT) for the simultaneous detection of the FRET donor and acceptor. All samples were excited through an oil objective (Olympus, UPlanSApo, 1.40 NA, 100×) with a 488-nm pulsed laser (PicoQuant, full width at half-maximum 120 ps) controlled by a PDL-800B driver (PicoQuant). An excitation power of about 33 μW was used.

dx.doi.org/10.1021/jp4036277 | J. Phys. Chem. B XXXX, XXX, XXX−XXX

DNA Preparation. ssDNA for FRET and FCS studies was purchased from JBios. The sequence is 5′-Cy3-TAGGG-$(TTAGGG)_3$-TT-Cy5-3′ (Cy3 was labeled to the 5′-end by a reaction with Cy3-NHS ester and 5′-N-TFE-amino modifier C6, and Cy5 to the 3′ end by a reaction with Cy5-maleimid and 3′-thiol modifier C3 S−S). For CD studies, 5′-TA GGG-$(TTAGGG)_3$-TT-3′ was synthesized on an Applied Biosystems 3400 DNA synthesizer with standard solid-phase techniques and purified on a JASCO HPLC with a reversed phase C-18 column with an acetonitrile/50 mM ammonium formate gradient. The DNAs were characterized by digestion with nuclease P1 and alkaline phosphatase and by MALDI-TOF mass spectra. DNA concentration was determined from the absorbance at 260 nm. The purity was confirmed by the rate of A_{260}/A_{280} = 1.83. In this study, we used 10 mM Tris-HCl buffer solutions (pH 7.4 at room temperature).

***E. coli* RecA Protein.** *E. coli* RecA, which is supplied in 10 mM Tris−HCl (pH 7.4 at 25 °C), 0.1 mM EDTA, 1 mM dithiothreitol, and 50% glycerol, was purchased from New England BioLabs. We used ATPγS (SIGMA-Aldrich) to avoid ATP hydrolysis and simplifying the interaction between DNA and RecA.

3. RESULTS AND DISCUSSION

Figure 2a shows changes in the fluorescence spectrum of **Cy5-G-q-Cy3** as a function of $[K^+]$. Upon addition of K^+ ions, the fluorescence intensity (I_A) of the acceptor (Cy5) attached to **G-q** was significantly enhanced, whereas the fluorescence intensity (I_D) of the donor (Cy3) was quenched to a large extent. This spectral change is due to the structural transition of **Cy5-G-q-Cy3** from ssDNA to G-quadruplex, resulting in the efficient FRET from donor (D) to acceptor (A). From the variation of the FRET efficiency (E_{FRET}, $I_A/(I_A + I_D)$) of **Cy5-G-q-Cy3** as a function of $[K^+]$, the transition midpoint is determined to be ~5 mM K^+ (Figure 2a). Moreover, the formation of G-quadruplex with the synthesized oligonucleotide in the presence of 100 mM K^+ ions was ensured by its characteristic CD spectrum, producing a positive band at 290 nm with a shoulder at 265 nm and a negative band at 236 nm (Figure 2b), indicating that G-quadruplex has mainly an antiparallel/parallel hybrid (3 + 1) structure. The observed CD spectrum for **Cy5-G-q-Cy3** is consistent with that reported by Heddi et al. and Ambrus et al.,[28,29] suggesting that the formation and structure of the G-quadruplex are unaffected by the covalent attachment of dyes.

To elucidate the interaction between the single-stranded/G-quadruplex **Cy5-G-q-Cy3** and RecA protein, we measured the CD spectrum of single-stranded and G-quadruplex **Cy5-G-q-Cy3** in the absence and presence of RecA (Figure 2b). Upon addition of RecA to ssDNA solution in the absence of K^+ ions, the positive band near 255 nm and the negative band near 240 nm, which are characteristic bands of unstructured ssDNA, are slightly blue-shifted with the decrease of the ellipticity, and the new CD band is observed at 295 nm. This spectral change is due to the formation of the RecA@ssDNA filament. As depicted in Figure 2b, however, the addition of 100 mM K^+ ions resulted in a significant change in the CD spectrum of RecA@ssDNA filament: the CD spectrum exhibited a positive band at 290 nm with a shoulder at 265 nm and a negative band at 236 nm, which is a characteristic of G-quadruplex with an antiparallel/parallel hybrid (3 + 1) structure (red line in Figure 2b). This observation indicates that the RecA@ssDNA filament is dissociated by the addition of K^+ ions, and subsequently the

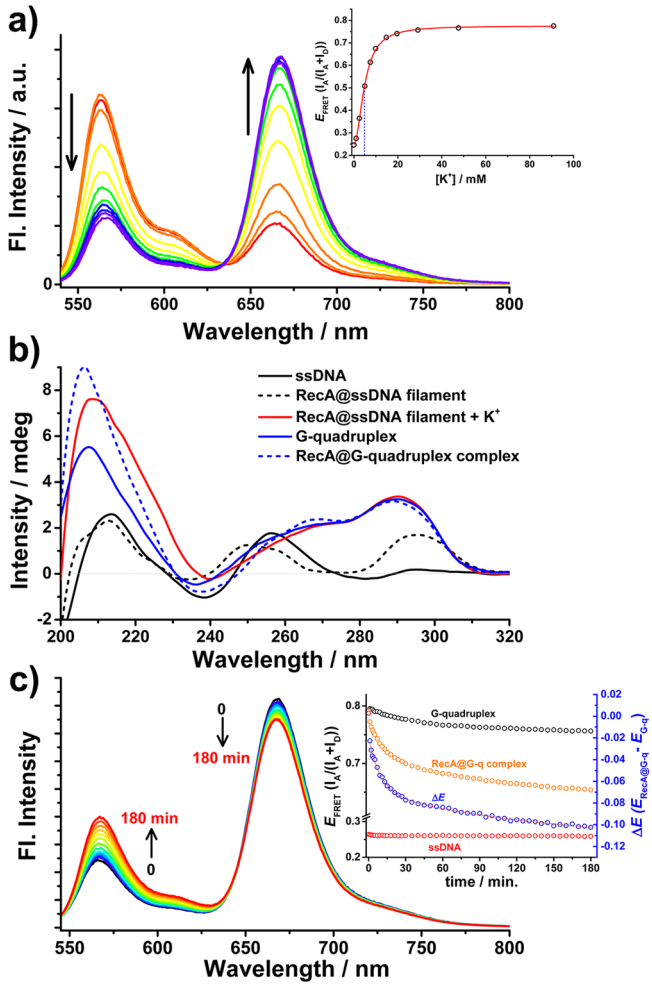

Figure 2. (a) Changes in the fluorescence spectrum of **Cy5-G-q-Cy3** as a function of $[K^+]$. ([**Cy5-G-q-Cy3**] = 84 nM; $[K^+]$ = 0 mM (red) ~ 100 mM (purple)). The inset shows changes in E_{FRET} for **Cy5-G-q-Cy3** as a function of $[K^+]$. Theoretical fit obtained from the fitting analysis is shown in red. (b) CD spectra of ssDNA and G-quadruplex ([DNA] = 20 μM) in the presence and absence of 10 μM RecA protein. (RecA@ssDNA filament: 20 μM ssDNA, 100 μM ATPγS, 10 mM $MgCl_2$, and 10 μM RecA; RecA@G-quadruplex complex: 20 μM ssDNA, 100 μM ATPγS, 10 mM $MgCl_2$, 10 μM RecA). The CD signal of RecA was subtracted from the CD signal of the DNA and RecA mixture sample. (c) Fluorescence spectra of the G-quadruplex **Cy5-G-q-Cy3** recorded at different times following addition of RecA (84 nM G-quadruplex, 100 mM KCl, 10 μM ATPγS, 10 mM $MgCl_2$, 1 μM RecA). The inset shows changes in E_{FRET} monitored at different times following the addition of RecA. The theoretical fitting curve for ΔE is shown in red.

dissociated ssDNA is converted to the G-quadruplex structure, suggesting that the G-quadruplex structure is more favorable than the RecA@ssDNA filament in the presence of K^+ ions. Furthermore, we found that the structural transition from the RecA@ssDNA filament to the G-quadruplex needs more K^+ ions compared with that from ssDNA to G-quadruplex in the absence of RecA protein. From the variation of E_{FRET} ($I_A/(I_A + I_D)$) of the RecA@ssDNA filament as a function of $[K^+]$, the transition midpoint is determined to be ~11 mM K^+ (Figure S1). Bar-Ziv et al. showed that the RecA protein strongly binds to pyrimidine-rich sequences (cytosine and thymine) with a high-affinity, whereas RecA binding with purine-rich sequences (adenine and guanine) is weaker and less cooperative because

dx.doi.org/10.1021/jp4036277 | J. Phys. Chem. B XXXX, XXX, XXX−XXX

purine-rich sequences have a strong base stacking and tight secondary structure compared with pyrimidine-rich sequences.[30] Thus, the structural transition from the RecA@ssDNA filament to the G-quadruplex upon addition of K^+ ions is probably due to the weak binding affinity between the RecA protein and the single-stranded G-rich sequence.

Meanwhile, the CD spectrum of the G-quadruplex formed with K^+ ions was affected little by the addition of RecA (Figure 2b), suggesting a small change in the conformation of the G-quadruplex by addition of RecA protein. Substantially, the CD spectra cannot distinguish the different species with similar physical properties.[31] To further investigate whether RecA protein binds to G-quadruplex, we measured the fluorescence spectra of G-quadruplex **Cy5-G-q-Cy3** recorded at different times following the addition of RecA. As shown in Figure 2c, the addition of RecA to the G-quadruplex **Cy5-G-q-Cy3** resulted in the enhancement of I_D, while reduction resulted in that of the I_A. The significant reduction of E_{FRET} means an increase in the D−A distance. In contrast to the G-quadruplex, the RecA@ssDNA filament shows constant values of E_{FRET} (Figure S2). This result suggests that the RecA protein substantially binds to the G-quadruplex and consequently forms the RecA@G-quadruplex complex. This is in contrast to the result obtained from the CD study on the interaction between G-quadruplex and RecA protein, supporting that the CD signal is not highly sensitive for the G-quadruplex-RecA interaction without a great conformational change of the G-quadruplex. Recently, Patel and co-workers revealed that in vitro, the three-layered all parallel-stranded *pilE* G-quadruplex containing single-residue double-chain reversal loops binds *E. coli* RecA protein, whereas the G-quadruplex with grooves connected by two- or three-residue double-chain reversal loops did not bind to the RecA protein because of steric clashes into the 3-nt DNA-binding site of RecA.[32] Their results imply that G-quadruplex with a different structure can bind to RecA protein in a different manner. Thus, we suggest that the change in E_{FRET} of **Cy5-G-q-Cy3** followed by the addition of RecA protein is due to the binding of RecA protein to G-quadruplex DNA, resulting in the formation of the RecA@G-quadruplex complex.

On the other hand, the kinetic aspect for interaction between G-quadruplex and RecA was monitored by the changes in E_{FRET} with respect to the time upon addition of RecA. The kinetic trace showed the relaxation dynamics with the time constant of 2×10^{-3} s^{-1} (Figure 2c), which probably reflects the binding of RecA protein to G-quadruplex and the subsequent conformational change of the RecA@G-quadruplex complex. Cazenave and co-workers reported that the rate constant of the nucleation-elongation process triggered by binding of RecA protein to single-stranded poly(deoxy-1,N^6-ethenoadenylic acid), poly(dεA), was 7×10^5 M^{-1} s^{-1} in the presence of ATPγS.[33] Considering the concentration of 84 nM G-quadruplex and the rate constant of 7×10^5 $M^{-1}s^{-1}$, the rate constant for the formation of the RecA@G-quadruplex complex is calculated to be 5.9×10^{-2} s^{-1}, which is in significant contrast with the experimental value of 2×10^{-3} s^{-1}. This discrepancy conceivably originated from the cooperative effect of the different affinity of RecA protein for G-quadruplex compared to poly(dεA) and the slow conformational change of G-quadruplex followed by the binding of RecA protein. In addition, we determined the binding ratio of the RecA@G-quadruplex complex using continuous variation analysis (Job plot) in FRET efficiency (E_{FRET}) (Figure 3). From the

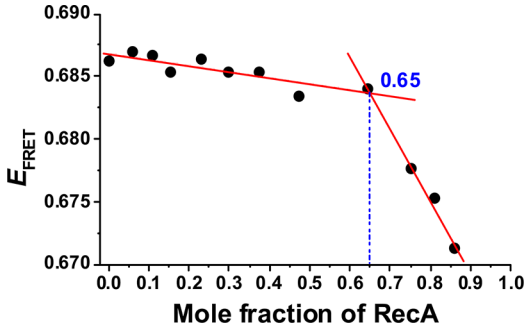

Figure 3. Job plot for RecA binding to G-quadruplex in the presence of 100 mM K+ ions. ([G-quadruplex] = 168 nM).

inflection point of ∼0.65, the number of RecA proteins bound per G-quadruplex is estimated to be about 2 RecA monomers. Considering the high-affinity of RecA protein for pyrimidine nucleotides and G-quadruplex structure, two RecA proteins may bind to two edgewise loops of G-quadruplex. The conformational change of G-quadruplex followed by the binding of RecA protein is further discussed in the following section.

Furthermore, the hydrodynamic radii of the RecA@ssDNA filament and the RecA@G-quadruplex complex at the single-molecule level are measured using FCS, and the results are shown in Figure 4. If G-quadruplex and ssDNA forms a

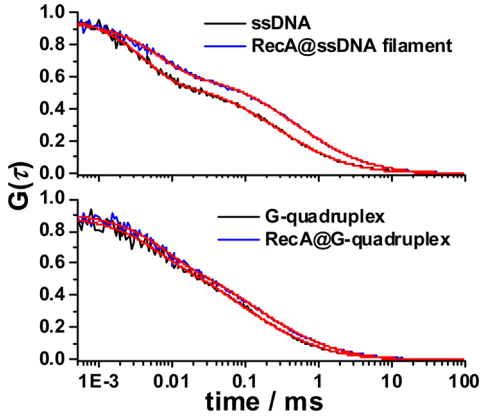

Figure 4. Normalized FCS curves of single-stranded and G-quadruplex **Cy5-G-q-Cy3** in the absence (black lines) and presence (blue lines) of RecA. Theoretical fits obtained from the fitting analysis are shown in red.

complex with RecA protein, respectively, its respective hydrodynamic radius should be larger than that of G-quadruplex and ssDNA. FCS has been accepted as a very useful tool to measure the translational diffusion of a biomolecule. The molecular diffusion time can provide not only information on the size and shape of biomolecules, but also on the intermolecular interaction between biomolecules.[34−39] Thus, the molecular diffusion time can directly provide information on the change in molecular size associated with the formation of RecA@ssDNA filament and RecA@G-quadruplex complex. In FCS, the autocorrelation function of the fluorescence intensity, $G(\tau)$, is given by

$$G(\tau) = \frac{\langle I(t)\cdot I(t+\tau)\rangle}{\langle I(t)\rangle^2} \quad (1)$$

dx.doi.org/10.1021/jp4036277 | J. Phys. Chem. B XXXX, XXX, XXX−XXX

where $I(t)$ is the fluorescence intensity at time t, $I(t + \tau)$ is the fluorescence intensity after a time lag τ, and $\langle\rangle$ denotes the time average over the total observation time. Figure 4 shows FCS curves of ssDNA and G-quadruplex in the absence and presence of RecA. All FCS curves show two dynamics: one is due to the fast relaxation process corresponding to singlet−triplet relaxation of Cy5, and the other is attributed to the translational diffusion of each chemical species. Thus, the autocorrelation function can be expressed by

$$G(\tau) = \frac{1}{N} \times \left\{ \left(1 + \frac{\tau}{\tau_d}\right)^{-1} \times \left[1 + \left(\frac{s}{u}\right)^2 \left(\frac{\tau}{\tau_d}\right)\right]^{-1/2} \right\} \times \left(1 + \frac{F}{1-F}\right) \exp\left(-\frac{\tau}{\tau_T}\right) \quad (2)$$

$$\frac{\tau_D'}{\tau_D} = \frac{\frac{s^2}{4D'}}{\frac{s^2}{4D}} = \frac{D}{D'} = \frac{R_h'}{R_h}\left(D = \frac{kT}{6\cdot\pi\cdot\eta\cdot R_h}\right) \quad (3)$$

where N is the average number of molecules in the observed volume, τ_d is the molecular diffusion time, s/u is the parameter to represent the shape of the observed volume, F is the fraction of the molecules in the triplet state, τ_T is the relaxation time of singlet−triplet relaxation, and D is the diffusion coefficient of a molecule. From the quantitative analysis of FCS curves with eq 2, the observed singlet−triplet relaxation time constants (τ_T) were calculated to be $0.13 - 0.23 \times 10^6$ s^{-1}, which is consistent with the previously reported values of $0.11 - 0.47 \times 10^6$ s^{-1},[40] indicating that the singlet−triplet relaxation of Cy5 is not affected by the site-specific labeling. The diffusion time (τ_d) of ssDNA and the G-quadruplex is determined to be 2.7 ± 0.1 and 1.8 ± 0.2 ms, respectively. As the τ_d is proportional to the hydrodynamic radius (R_h) of a molecule (eq 3), the decrease of τ_d followed by the structural change from ssDNA to G-quadruplex means that there was a decrease of the hydrodynamic radius by 0.67 times ($R_{h\text{-G-quadruplex}}/R_{h\text{-ssDNA}} = 0.67$). The similar result was observed for i-motif DNA, which has a tetraplex structure.[34] The decrease of the hydrodynamic radius followed by the structural change from ssDNA to G-quadruplex is mainly due to the change in the molecular shape from a random coil structure to tetraplex structure with a spherical shape. Meanwhile, the τ_d values of the RecA@ssDNA filament and the RecA@G-quadruplex complex are determined to be 4.9 ± 0.2 and 2.6 ± 0.3 ms, respectively. These observations imply that the R_h's of the RecA@ssDNA filament and the RecA@G-quadruplex complex are ∼1.8 and ∼1.5 times larger than those of the ssDNA and G-quadruplex, respectively. These significant changes in R_h's support that the G-quadruplex as well as ssDNA substantially bind to RecA protein.

As the τ_d is related to the molecular weight of a molecule (eq 4), τ_d'/τ_d is given by

$$\frac{\tau_d'}{\tau_d} = \left(\frac{M'}{M}\right)^{1/3} \quad (4)$$

where τ_d' and τ_d are the molecular diffusion time of RecA@ssDNA filament (or RecA@G-quadruplex complex) and ssDNA (or G-quadruplex), respectively. M' and M are the molecular weight of RecA@ssDNA filament (or RecA@G-quadruplex) and ssDNA (or G-quadruplex), respectively. It is well-known that the helical RecA@ssDNA filament has ∼6.2 RecA proteins per turn—approximately 3−4 nt per RecA protein.[41,42] On the other hand, from the Job plot, we showed that two RecA proteins bind to two edgewise loops of G-quadruplex. Therefore, 2 RecA proteins can bind to one G-quadruplex DNA, whereas ∼7 RecA proteins bind to one ssDNA sequence. Considering the molecular weight of RecA (∼38 kDa) and **Cy5-G-q-Cy3** (∼9.6 kDa), the theoretical R_h's of the RecA@ssDNA filament and RecA@G-quadruplex complex should be ∼2.9 and 2.1 times larger than that of ssDNA and G-quadruplex, respectively. However, the measured R_h's for the RecA@ssDNA filament and RecA@G-quadruplex complex are significantly smaller than values expected from the molecular weight. A similar result was reported by Cohen and co-workers.[37] The different nucleoprotein structure including bent or curved filament or the transient dissociation of RecA monomer from the RecA@ssDNA filament or RecA@G-quadruplex complex can induce the decrease of its R_h. However, the ssDNA used in this study is a short 25-mer DNA sequence, and consequently, the RecA@ssDNA filament may have a rigid rod-like shape. In addition, the RecA@G-quadruplex complex may have a spherical structure because both G-quadruplex and RecA protein have a spherical structure in solutions. Moreover, we used ATPγS instead of ATP to prevent the dissociation of RecA monomer, ensuring the possibility of decrease in R_h due to the transient dissociation of RecA monomer. Therefore, the decrease of R_h due to the different nucleoprotein structure or the transient dissociation of RecA monomer from the RecA@ssDNA filament (or RecA@G-quadruplex complex) can be ruled out. From these reasons, we also suggest that the discrepancy comes from the changes in net charge or Stokes drag, which can affect the translational diffusion of a molecule. Meanwhile, we cannot rule out the possibility that observed small changes in the τ_d for both RecA@ssDNA filament and RecA@G-quadruplex complex are due to the low sensitivity of the FCS measurements. Practically, the sensitivity of the FCS measurement on the molecular (protein−DNA complex) mass changes is not particularly sensitive. From simple math using eq 4, 10-fold increases in molecular weight will produce 2.15-fold increases in the τ_d. This may be why the measured τ_d's for the RecA@ssDNA filament and RecA@G-quadruplex complex are significantly smaller than values expected from the molecular weight.

Finally, changes in the FRET efficiency of freely diffusing ssDNA and G-quadruplex in the absence and presence of RecA protein were also measured at the single-molecule level. Single-molecule fluorescence spectroscopy provides an insight into the behavior of each individual molecule and consequently allows a detailed observation of subpopulations in structures or dynamics hidden under ensemble-averaged results.[43−45] As depicted in Figure 5, the E_{FRET} histogram for ssDNA in the absence of RecA shows a broad and single FRET peak centered at 0.32 caused by various conformational isomers due to its flexible structure. By contrast, the E_{FRET} histogram of RecA@ssDNA filament shows a narrow single FRET peak centered at 0.29. As mentioned above, the RecA@ssDNA filament has an elongated and rigid rod-like shape, resulting in the decrease of the E_{FRET} and conformational heterogeneities in ssDNA. Meanwhile, G-quadruplex in the absence of RecA shows a broad peak consisting of two peaks (0.69 and 0.86), indicating that there are at least two species in this system: one is a structural species with E_{FRET} of 0.69 as a major species (83%), and the other is a different G-quadruplex structure with E_{FRET} of 0.86 as a minor species (17%). Phan et al. showed that the human telomeric **G-q** sequence adopts two intramolecular (3 +

dx.doi.org/10.1021/jp4036277 | J. Phys. Chem. B XXXX, XXX, XXX−XXX

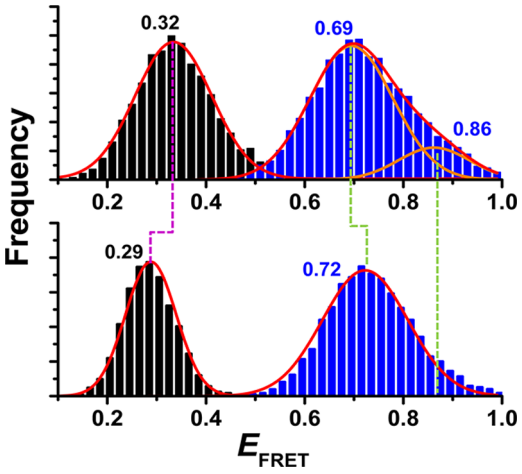

Figure 5. FRET efficiency distributions of single-stranded and G-quadruplex **Cy5-G-q-Cy3** in the absence (top panel) and presence (bottom panel) of RecA. Red solid lines denote Gaussian fitting curves.

1) G-quadruplexes in the presence of K^+ ions, which differ from each other only by the order of loop arrangement.[46] The NMR structure revealed that both the 3′- and 5′-ends in the G-quadruplex structure with two double-chain-reversal loops are in the nearby location, while the 3′- and 5′-ends in another species with one double-chain-reversal loop are far apart.[46] Considering two intramolecular (3 + 1) G-quadruplex structures and the observed E_{FRET}, the major species observed in this study has a structure with one double-chain-reversal loop, whereas the minor species is attributed to G-quadruplex with two double-chain-reversal loops. Interestingly, upon addition of RecA, the FRET efficiency distribution of G-quadruplex shows a narrow single FRET peak centered at 0.72 with the disappearance of G-quadruplex structure with E_{FRET} of 0.86, implying that the reduction of the multiplicity of the G-quadruplex structure. The disappearance of G-quadruplex (E_{FRET} ~0.86) with double-chain-reversal loops upon addition of RecA protein implies that the binding of RecA to G-quadruplex with two double-chain-reversal loops induces the structural change to G-quadruplex with one double-chain-reversal loop. That is, RecA protein forms the more stable complex with G-quadruplex, which has one double-chain-reversal and two edgewise loops.

4. CONCLUSIONS

In this study, we investigated the interaction between RecA protein and a G-rich sequence in bulk phase and at the single-molecule level. The result presented here show that the G-quadruplex structure is more favorable than the RecA@ssDNA filament in the presence of K^+ ions (Figure 6). Furthermore, we clearly show that the binding of RecA protein to the conformationally heterogeneous G quadruplex induces the structural change into the specific structure of G-quadruplex with one double-chain-reversal loop. Recently, Patel and co-workers showed that the binding of RecA protein to *pilE* G-quadruplex promotes *E. coli* RecA-mediated strand exchange in vitro.[32] Thus, we believe this will certainly contribute to the further understanding of the protein−DNA interaction occurring in biological systems.

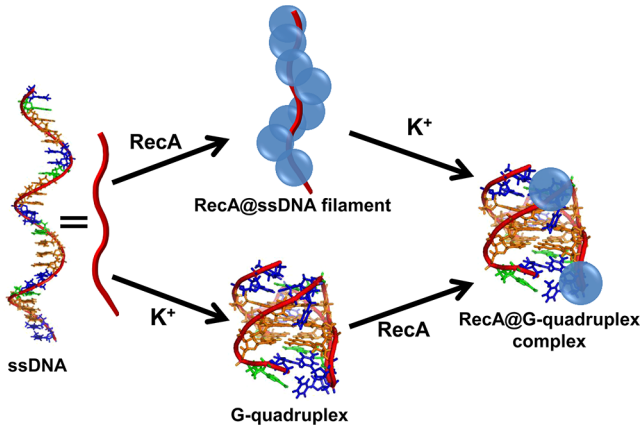

Figure 6. Schematic illustration of the interaction between RecA protein and G-rich DNA.

■ ASSOCIATED CONTENT

Supporting Information

Detailed description of materials and methods, and additional results. This material is available free of charge via the Internet at http://pubs.acs.org.

■ AUTHOR INFORMATION

Corresponding Author

*E-mail: jkchoi@sanken.osaka-u.ac.jp (J.C.); majima@sanken.osaka-u.ac.jp (T.M.).

Notes

The authors declare no competing financial interest.

■ ACKNOWLEDGMENTS

This work has been partly supported by the Innovative Project for Advanced Instruments, Renovation Center of Instruments for Science Education and Technology, Osaka University, and a Grant-in-Aid for Scientific Research (Projects 22245022, 24550188, and others) from the Ministry of Education, Culture, Sports, Sciences and Technology (MEXT) of Japanese Government. T. M. thanks the World Class University program funded by the Ministry of Education, Science and Technology through the National Research Foundation of Korea (R31-2011-000-10035-0) for support. S.K.K. acknowledges partial support for this work by the Korea Research Foundation (Grant No. 2012-008875).

■ REFERENCES

(1) Lusetti, S. L.; Cox, M. M. The Bacterial RecA Protein and the Recombinational DNA Repair of Stalled Replication Forks. *Annu. Rev. Biochem.* **2002**, *71*, 71−100.

(2) Shan, Q.; Cox, M. M. RecA Filament Dynamics during DNA Strand Exchange Reactions. *J. Biol. Chem.* **1997**, *272*, 11063−11073.

(3) Fulconis, R.; Mine, J.; Bancaud, A.; Dutreix, M.; Viovy, J. L. Mechanism of RecA-Mediated Homologous Recombination Revisited by Single Molecule Nanomanipulation. *EMBO J.* **2006**, *25*, 4293−4304.

(4) Takahashi, M.; Maraboeuf, F.; Morimatsu, K.; Selmane, T.; Fleury, F.; Norden, B. Calorimetric Analysis of Binding of Two Consecutive DNA Strands to RecA Protein Illuminates Mechanism for Recognition of Homology. *J. Mol. Biol.* **2007**, *365*, 603−611.

(5) Chen, Z.; Yang, H.; Pavletich, N. P. Mechanism of Homologous Recombination from the RecA-ssDNA/dsDNA Structures. *Nature* **2008**, *453*, 489−484.

(6) Williams, R. C.; Spengler, S. J. Fibers of RecA Protein and Complexes of RecA Protein and Single-Stranded φX174 DNA as

Visualized by Negative-Stain Electron Microscopy. *J. Mol. Biol.* **1986**, *187*, 109−118.
(7) Bryant, F. R.; Taylor, A. R.; Lehman, I. R. Interaction of the RecA Protein of *Escherichia coli* with Single-Stranded DNA. *J. Biol. Chem.* **1985**, *260*, 1196−1202.
(8) Stasiak, A.; Di Capua, E.; Koller, T. Elongation of Duplex DNA by RecA Protein. *J. Mol. Biol.* **1981**, *151*, 557−564.
(9) Muller, B.; Koller, T.; Stasiak, A. Characterization of the DNA Binding Activity of Stable RecA-DNA Complexes. Interaction between the Two DNA Binding Sites within RecA Helical Filaments. *J. Mol. Biol.* **1990**, *212*, 97−112.
(10) Joo, C.; McKinney, S. A.; Nakamura, M.; Rasnik, I.; Myong, S.; Ha, T. Real-Time Observation of RecA Filament Dynamics with Single Monomer Resolution. *Cell* **2006**, *126*, 515−527.
(11) Ragunathan, K.; Joo, C.; Ha, T. Real-Time Observation of Strand Exchange Reaction with High Spatiotemporal Resolution. *Structure* **2011**, *19*, 1064−1073.
(12) Galletto, R.; Amitani, I.; Baskin, R. J.; Kowalczykowski, S. C. Direct Observation of Individual RecA Filaments Assembling on Single DNA Molecules. *Nature* **2006**, *443*, 875−878.
(13) Hwang, H.; Kim, H.; Myong, S. Protein Induced Fluorescence Enhancement as a Single Molecule Assay with Short Distance Sensitivity. *Proc. Natl. Acad. Sci. U.S.A.* **2011**, *108*, 7414−7418.
(14) Lander, E. S. Initial Sequencing and Analysis of the Human Genome. *Nature* **2001**, *409*, 860−921.
(15) Choi, J.; Majima, T. Conformational Changes of Non-B DNA. *Chem. Soc. Rev.* **2011**, *40*, 5893−5909.
(16) Zhao, J.; Bacolla, A.; Wang, G.; Vasquez, K. M. Non-B DNA Structure-Induced Genetic Instability and Evolution. *Cell. Mol. Life Sci.* **2010**, *67*, 43−62.
(17) Bacolla, A.; Wells, R. D. Non-B DNA Conformations as Determinants of Mutagenesis and Human Disease. *Mol. Carcinog.* **2009**, *48*, 273−285.
(18) Wang, G.; Vasquez, K. M. Non-B DNA Structure-Induced Genetic Instability. *Mutat. Res.* **2006**, *598*, 103−119.
(19) Huppert, J. L. Structure, Location and Interactions of G-quadruplexes. *FEBS J.* **2010**, *277*, 3452−3458.
(20) Wu, Y.; Brosh, R. M., Jr. G-Quadruplex Nucleic Acids and Human Disease. *FEBS J.* **2010**, *277*, 3470−3488.
(21) Lipps, H. J.; Rhodes, D. G-Quadruplex Structures: In Vivo Evidence and Function. *Trends Cell Biol.* **2009**, *19*, 414−422.
(22) Yu, H.; Gu, X.; Nakano, S.-i.; Miyoshi, D.; Sugimoto, N. Beads-on-a-String Structure of Long Telomeric DNAs under Molecular Crowding Conditions. *J. Am. Chem. Soc.* **2012**, *134*, 20060−20069.
(23) Lane, A. N.; Chaires, J. B.; Gray, R. D.; Trent, J. O. Stability and Kinetics of G-Quadruplex Structures. *Nucleic Acids Res.* **2008**, *36*, 5482−5515.
(24) Neidle, S. The Structures of Quadruplex Nucleic Acids and Their Drug Complexes. *Curr. Opin. Struct. Biol.* **2009**, *19*, 239−250.
(25) Balasubramanian, S.; Neidle, S. G-Quadruplex Nucleic Acids as Therapeutic Targets. *Curr. Opin. Chem. Biol.* **2009**, *13*, 345−353.
(26) Biffi, G.; Tannahill, D.; McCafferty, J.; Balasubramanian, S. Quantitative Visualization of DNA G-Quadruplex Structures in Human Cells. *Nat. Chem.* **2013**, *5*, 182−186.
(27) Story, R. M.; Weber, I. T.; Steitz, T. A. The Structure of the *E. coli* RecA Protein Monomer and Polymer. *Nature* **1992**, *355*, 318−325.
(28) Heddi, B.; Phan, A. T. Structure of Human Telomeric DNA in Crowded Solution. *J. Am. Chem. Soc.* **2011**, *133*, 9824−9833.
(29) Ambrus, A.; Chen, D.; Dai, J.; Bialis, T.; Jones, R. A.; Yang, D. Human Telomeric Sequence Forms a Hybrid-Type Intramolecular G-Quadruplex Structure with Mixed Parallel/Antiparallel Strands in Potassium Solution. *Nucleic Acids Res.* **2006**, *34*, 2723−2735.
(30) Bar-Ziv, R.; Libchaber, A. Effects of DNA Sequence and Structure on Binding of RecA to Single-Stranded DNA. *Proc. Natl. Acad. Sci. U.S.A.* **2001**, *98*, 9068−9073.
(31) Dailey, M. M.; Miller, M. C.; Bates, P. J.; Lane, A. N.; Trent, J. O. Resolution and Characterization of the Structural Polymorphism of a Single Quadruplex-Forming Sequence. *Nucleic Acids Res.* **2010**, *38*, 4877−4888.
(32) Kuryavyi, V.; Cahoon, L. A.; Seifert, H. S.; Patel, D. J. RecA-Binding pilE G4 Sequence Essential for Pilin Antigenic Variation Forms Monomeric and 5′ End-Stacked Dimeric Parallel G-Quadruplexes. *Structure* **2012**, *20*, 2090−2102.
(33) Chabbert, M.; Cazenave, C.; Helene, C. Kinetic Studies of RecA Protein Binding to a Fuorescent Single-Stranded Polynucleotide. *Biochemistry* **1987**, *26*, 2218−2225.
(34) Choi, J.; Kim, S.; Tachikawa, T.; Fujitsuka, M.; Majima, T. pH-Induced Intramolecular Folding Dynamics of i-Motif DNA. *J. Am. Chem. Soc.* **2011**, *133*, 16146−16153.
(35) Kim, S.; Choi, J.; Majima, T. Self-Assembly of Polydeoxyadenylic Acid Studied at the Single-Molecule Level. *J. Phys. Chem. B* **2011**, *115*, 15399−15405.
(36) Choi, J.; Kim, S.; Tachikawa, T.; Fujitsuka, M.; Majima, T. Unfolding Dynamics of Cytochrome c Revealed by Single-Molecule and Ensemble-Averaged Spectroscopy. *Phys. Chem. Chem. Phys.* **2011**, *13*, 5651−5658.
(37) Fields, A. P.; Cohen, A. E. Electrokinetic Trapping at the One Nanometer Limit. *Proc. Natl. Acad. Sci. U.S.A.* **2011**, *108*, 8937−8942.
(38) Kim, S. A.; Heinze, K. G.; Schwille, P. Fluorescence Correlation Spectroscopy in Living Cells. *Nat. Methods* **2007**, *4*, 963−973.
(39) Lakowicz, J. R. *Principles of Fluorescence Spectroscopy*, 3rd ed.; Springer: New York, 2006.
(40) Widengren, J.; Schwille, P. Characterization of Photoinduced Isomerization and Back-Isomerization of the Cyanine Dye Cy5 by Fluorescence Correlation Spectroscopy. *J. Phys. Chem. A* **2000**, *104*, 6416−6428.
(41) Bell, C. E. Structure and Mechanism of *Escherichia coli* RecA ATPase. *Mol. Microbiol.* **2005**, *58*, 358−366.
(42) McGrew, D. A.; Knight, K. L. Molecular Design and Functional Organization of the RecA Protein. *Crit. Rev. Biochem. Mol. Biol.* **2003**, *38*, 385−432.
(43) Lu, H. P. In *Single Molecule Spectroscopy in Chemistry, Physics and Biology*; Gräslund, A., Rigler, R., Widengren, J., Eds.; Springer: Berlin Heidelberg, 2010; Vol. *96*, p 471−494.
(44) Lee, J.; Lee, S.; Ragunathan, K.; Joo, C.; Ha, T.; Hohng, S. Single-Molecule Four-Color FRET. *Angew. Chem., Int. Ed. Engl.* **2010**, *49*, 9922−9925.
(45) Choi, J.; Tachikawa, T.; Kim, Y.; Fujitsuka, M.; Ihee, H.; Majima, T. Photophysical Properties of Zn-Substituted Cytochrome *c* Investigated by Single-Molecule and Ensemble-Averaged Spectroscopy. *Chem. Commun.* **2010**, *46*, 9155−9157.
(46) Phan, A. T.; Luu, K. N.; Patel, D. J. Different Loop Arrangements of Intramolecular Human Telomeric (3 + 1) G-Quadruplexes in K^+ Solution. *Nucleic Acids Res.* **2006**, *34*, 5715−5719.